Talanta 117 (2013) 258–262

Contents lists available at ScienceDirect

Talanta

journal homepage: www.elsevier.com/locate/talanta

One-pot synthesis of two-sized clusters for ratiometric sensing of Hg^{2+}

Tzu-Heng Chen [a,c], Chi-Yu Lu [b,c], Wei-Lung Tseng [a,c,d,*]

[a] Department of Chemistry, National Sun Yat-sen University, Taiwan
[b] Department of Biochemistry, College of Medicine, Kaohsiung Medical University, Taiwan
[c] School of Pharmacy, College of Pharmacy, Kaohsiung Medical University, Taiwan
[d] Center for Nanoscience and Nanotechnology, National Sun Yat-sen University, Taiwan

ARTICLE INFO

Article history:
Received 29 May 2013
Received in revised form
27 August 2013
Accepted 31 August 2013
Available online 9 September 2013

Keywords:
Ratiometric sensing
Gold nanoclusters
Mercury(II)
Fluorescence

ABSTRACT

This paper presents a discussion of a one-pot approach for preparing lyszoyme type VI (Lys VI) stabilized clusters, including small (Au_7Ag and Au_8) and large ($Au_{24}Ag$) clusters, for ratiometric fluorescence sensing of Hg^{2+}. Our previous study (Chen and Tseng, Small 8 (2012) 1912) showed the formation of intermediate Au_8 clusters in the conversion of Au^+–Lys VI protein complexes to Au_{25} clusters. The presence of Ag^+ in the precursor solution slowed this conversion, thereby forming two-sized clusters. With an increase in Ag^+ content, a systematic blue shift in the first exciton absorption and fluorescence peaks indicated the formation of Au–Ag bimetallic clusters. The prepared Ag^+/Au^{3+} molar ratio of 2:8 resulted in the formation of two-sized clusters, with dual emission bands centered at 471 and 613 nm. After these clusters are separated by a membrane filter, matrix-assisted laser desorption/ionization time-of-flight mass spectrometry was used to determine the composition of $Au_{24}Ag$ clusters. By monitoring the intensity ratio of the two emission wavelengths, the solution consisting of Hg^{2+}-insensitive small clusters (Au_7Ag and Au_8) and Hg^{2+}-sensitive $Au_{24}Ag$ clusters exhibited a ratiometric fluorescence response toward Hg^{2+}, and provided a built-in correction for photobleaching; the limit of detection at a signal-to-noise ratio of three for Hg^{2+} was estimated to be 1 nM. This probe was successfully applied to ratiometric fluorescence sensing of Hg^{2+} in tap water.

1. Introduction

The release of mercury into the aquatic environment is a global problem because of its lethal effects on the environment and human health. Sensors have been devised for simple, fast, cost-efficient detection of Hg^{2+} using fluorophores [1], chromophores [1], conjugated polymers [2], thymine-rich oligonucleotides [3], DNAzymes [4], semiconductor quantum dots [5], and gold nanoparticles [6]. Recently, gold nanoclusters (AuNCs) consisting of a few Au atoms have attracted attention as an emerging material for Hg^{2+} sensing because of the quenching of their fluorescence. Huang et al. synthesized 11-mercaptoundecanoic acid-capped AuNCs by etching large Au nanoparticles with thiols, and showed them to be capable of sensing Hg^{2+} through coordination between the carboxylic group of 11-mercaptoundecanoic acid and Hg^{2+} [7]. This coordination induced the aggregation of AuNCs, resulting in their fluorescence quenching. Xie et al. prepared red-emitting Au_{25} clusters through the reduction of $HAuCl_4$ with bovine serum albumin (BSA), and applied them to the detection of Hg^{2+} based on the formation of metallophilic bonds between Hg^{2+} ($4f^{14}5d^{10}$) and Au^+ ($4f^{14}5d^{10}$) [8]. This strong metallophilic bond enables BSA-stabilized Au_{25} clusters to be sensitive and provides selective detection of Hg^{2+}. Along with identical closed-shell interaction, Lin and Tseng reported that the fluorescence quenching of lysozyme type VI (Lys VI) stabilized Au_{25} clusters occurred not only in the presence of Hg^{2+}, but also in CH_3Hg^+ [6]. This probe was successful in detecting both ions in seawater. Although the above-mentioned sensors provided high sensitivity and selectivity toward Hg^{2+}, factors such as environmental conditions, the probe concentration, photobleaching, and the stability of the light source may interfere with their signal output. Theoretically, these problems can be circumvented using the ratiometric fluorescence technique, which is capable of sensing numerous analytes, such as heavy metals, anions, DNA, and chemical warfare agents [9–12]. Because this technique permits the measurement of the analyte by comparing the ratio of the fluorescent intensities at two wavelengths, it provides a build-in correction for the effects of environmental variation and the changes of probe concentration. However, no study reported that Hg^{2+} could be detected using an AuNC-based ratiometric fluorescence sensor.

This study develops a novel ratiometric sensor for the quantification of Hg^{2+} using two-sized metal clusters. When Lys VI serves as a template to prepare Au_{25} clusters at alkaline pH, the complexes

* Corresponding author at: Department of Chemistry, National Sun Yat-sen University, 70, Lien-hai Road, Kaohsiung 804, Taiwan. Tel.: +886 7 5254644; fax: +886 7 3684046.
E-mail address: tsengwl@mail.nsysu.edu.tw (W.-L. Tseng).

0039-9140/$ - see front matter © 2013 Elsevier B.V. All rights reserved.
http://dx.doi.org/10.1016/j.talanta.2013.08.057

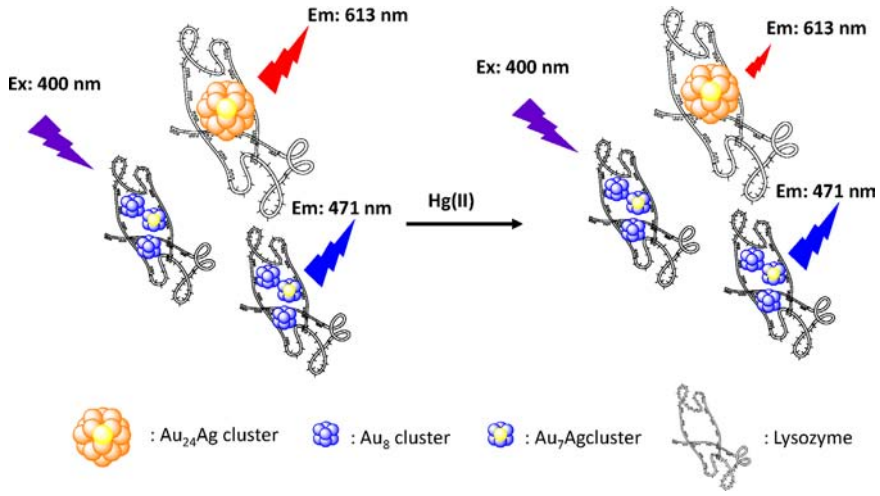

Scheme 1. Illustration of the mechanism of two-sized clusters for sensing Hg^{2+}.

of Lys VI and Au^{3+} are initially reduced to Au_8 clusters with tyrosine residue [13]. The intermediate Au_8 clusters continued to convert to Au_{25} clusters. In contrast, the presence of Ag^+ slows this conversion because of the underpotential deposition of Ag onto the Au surface (Scheme 1B) [14–16]. The phenomenon of underpotential deposition occurs because an existing Au surface enables the reduction of Ag^+ at a potential that is less negative than the Nernst potential. Under optimal time and $AgNO_3$ concentration, the reacted solution simultaneously contains small and large clusters. Previous studies have shown that Hg^{2+} was capable of quenching the fluorescence of Au_{25} clusters, but not that of the Au_8 clusters [13]. Because the solution consists of Hg^{2+}-insensitive small (Au_7Ag and Au_8) clusters and Hg^{2+}-sensitive $Au_{24}Ag$ clusters, we were able to design a ratiometric fluorescent probe for Hg^{2+}. Scheme 1 schematically depicts the design concept.

2. Materials and methods

2.1. Chemicals

Lys VI (chicken eggwhite) was ordered from MP Biomedicals (Irvine, CA). $HAuCl_4$ was ordered from Alfa aesar (Ward Hill, MD, USA). NaOH, NaCl, KCl, $MgCl_2$, $CaCl_2$, $BaCl_2$, $CrCl_3$, $FeCl_2$, $FeCl_3$, $CoCl_2$, $NiCl_2$, $CuCl_2$, $ZnCl_2$, $MnCl_2$, AgCl, $Cd(ClO_4)_2$, $Pb(NO_3)_2$, and $HgCl_2$ were obtain from Acros (Geel, Belgium). $AgNO_3$, LiCl, Na_2MoO_4, and $SrCl_2$ were purchased from Sigma-Aldrich (St. Louis, MO). Milli-Q ultrapure water (Milli-pore, Hamburg, Germany) was used in all of the experiments.

2.2. Instrumentation

The absorption and fluorescence spectra of Au_7Ag and $Au_{24}Ag$ clusters were obtained using a double-beam UV–visible spectrophotometer (Cintra 10e; GBC, Victoria, Australia) and a Hitachi F-7000 fluorometer (Hitachi, Tokyo, Japan), respectively. 100 kDa Nanosep centrifugal device (Pall Co., East Hills, NY) was used to separate a mixture of Au_7Ag and $Au_{24}Ag$ clusters. The molecular weights of Au_7Ag and $Au_{24}Ag$ clusters were determined by the Autoflex matrix-assisted laser desorption/ionization time-of-flight mass spectrometry (MALDI-TOF MS; Bruker Daltonics, Germany). Before MALDI-TOF MS measurement, saturated 2,5-dihydroxybenzoic acid containing 70% acetonitrile was added to a solution of the purified metal clusters. We pipetted the resulting mixtures onto a stainless steel 384-well target (Bruker Daltonics, Germany) and dried them at room temperature.

2.3. Synthesis of two-sized clusters

A solution of 25 mg/mL Lys VI was added to an equal volume of a mixture of 0–10 mM $AgNO_3$ and 0–10 mM $HAuCl_4$. The pH of the mixed solutions was adjusted to 12 with 1 M NaOH. The resulting solutions were incubated at 37 °C for 18 h.

2.4. Ratiometric sensing

Hg^{2+} (300 μL, 6 nM–10 μM) and other metal ions (300 μL, 5 μM) were separately added to an equal volume of two-sized metal clusters. The mixed solutions were incubated at ambient temperature for 15 min, and then transferred into 1 mL quartz cuvette. Their fluorescence spectra were recorded by operating the fluorescence spectrophotometer at an excitation wavelength of 400 nm.

2.5. Determination of Hg(II) in tap water

Tap water samples were collected from our campus. A series of samples were prepared by spiking them with standard solutions of Hg^{2+} (0–10 μM). The resulting solution was added to an equal volume of two-sized metal clusters. After 15 min, their fluorescence spectra were recorded at an excitation wavelength of 400 nm. Also, the concentration of Hg^{2+} in tap water was measured by inductively coupled plasma mass spectroscopy (ICP-MS; Perkin Elmer-SCIEX, Thornhill, ON, Canada).

3. Results and discussion

3.1. Characterization of large and small bimetallic clusters

The composition and optical properties of Au–Ag bimetallic clusters relies on the Au/Ag molar ratio in the precursor solution, and the intrinsic reactivity of Au and Ag toward a reducing agent [17–19]. Lys VI has been shown as both a reducing and a stabilizing agent for producing blue-emitting Au_8 clusters and red-emitting Au_{25} clusters at pH 3 and 12, respectively [13]. We prepared a series of mixtures of Lys VI (25 mg/mL), $HAuCl_4$, and $AgNO_3$, with different molar ratios of Ag^+-to-Au^{3+} at a constant total concentration (10 mM) of Au^{3+} and Ag^+. To ensure reaction completion, reaction time was fixed at 18 h. Fig. S1 (Supplementary information) shows that the as-prepared solutions all exhibited the absence of localized surface plasmon resonance bands, indicating the formation of metallic or bimetallic clusters. An increase in the Ag^+ concentration resulted in a systematic blue shift in the absorption edge and maximum

fluorescence emission, reflecting the formation of Au–Ag bimetallic clusters (Figs. S1 and S2, Supplementary information). Similar phenomena were observed in the preparation of 11-mercaptoundecanoic acid-, tiopronin-, and protein-capped Au–Ag bimetallic clusters [17–19]. Fig. S3 (Supplementary information) shows that the prepared Ag^{+}-to-Au^{3+} ratios of 2:8 had the highest quantum yields compared to other Au–Ag bimetallic clusters, Ag clusters, and Au clusters. The quantum yield of the formed clusters was determined using Rhodamine 6G as the reference. Wu et al. stated that the presence of Ag^{+} can cause the enhancement in the fluorescence of glutathione-capped Au^{25} clusters [20]. Huang et al. reported that the addition of Ag^{+} to the precursor solution can increase the fluorescence of 11-mercaptoundecanoic acid-capped AuNCs [17]. We suggest that the fluorescence enhancement could be attributed to the replacement of Au sites in AuNCs by Ag atoms, thereby forming stable bimetallic clusters.

The prepared Ag^{+}-to-Au^{3+} ratio of 2:8 shows dual emission bands centered at 471 and 613 nm upon excitation at 400 nm (curve a in Fig. 1). We suspected that two-sized clusters were produced in one pot. To confirm this hypothesis, a membrane filter with 100 kDa was used to separate a mixture of small and large clusters. After centrifugal ultrafiltration, the obtained solution containing small clusters was examined using fluorometer and MALDI-TOF MS. Curve b in Fig. 1 shows that small clusters exhibited blue fluorescence maximized at 471 nm, suggesting the presence of Au_8 or $Au_{8-n}Ag_n$ clusters through the prediction of the spherical Jellium model [21]. This emission wavelength was near to that reported for polyethylenimine-protected (λ_{em}= 455 nm) [22], Lys VI-stabilized (λ_{em}=455 nm) [13], and poly (amidoamine) dendrimer-encapsulated (λ_{em}=458 nm) Au_8 clusters [23]. Because proteins containing aromatic acid residues can exhibit a blue emission upon excitation at 400 nm, we compared the fluorescence spectra of Lys VI and small clusters. Fig. S4 (Supplementary information) shows that the fluorescence of small clusters is much stronger than that of Lys VI, indicating that the blue emission originated from small clusters, rather than from Lys VI.

Fig. 2A displays that the MALDI-TOF mass spectrum of small clusters is composed of peaks from *m/z* 14,000 to 16,000, compared to the mass spectrum of Lys VI (Fig. S5, Supplementary information). The difference in the molecular weight between Lys VI-stabilized clusters and Lys VI shows the formation of metallic or bimetallic clusters. MALDI-TOF MS was also used for the analysis of large clusters. The MALDI-TOF mass spectrum of large clusters consisted of four major peaks with a spacing of *m/z* 197 (Fig. 2B). These peaks appearing at *m/z* 4638, 4835, 5032, and 5229 were assigned to $[Au_{23}Ag]^{+}$, $[Au_{24}Ag]^{+}$, $[Au_{25}Ag]^{+}$, and $[Au_{26}Ag]^{+}$,

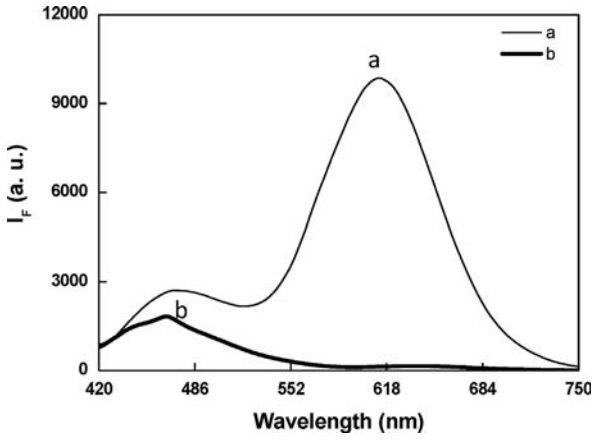

Fig. 1. Fluorescence spectra of a solution of two-sized clusters (a) before and (b) after the treatment with a membrane filter (100 kDa).

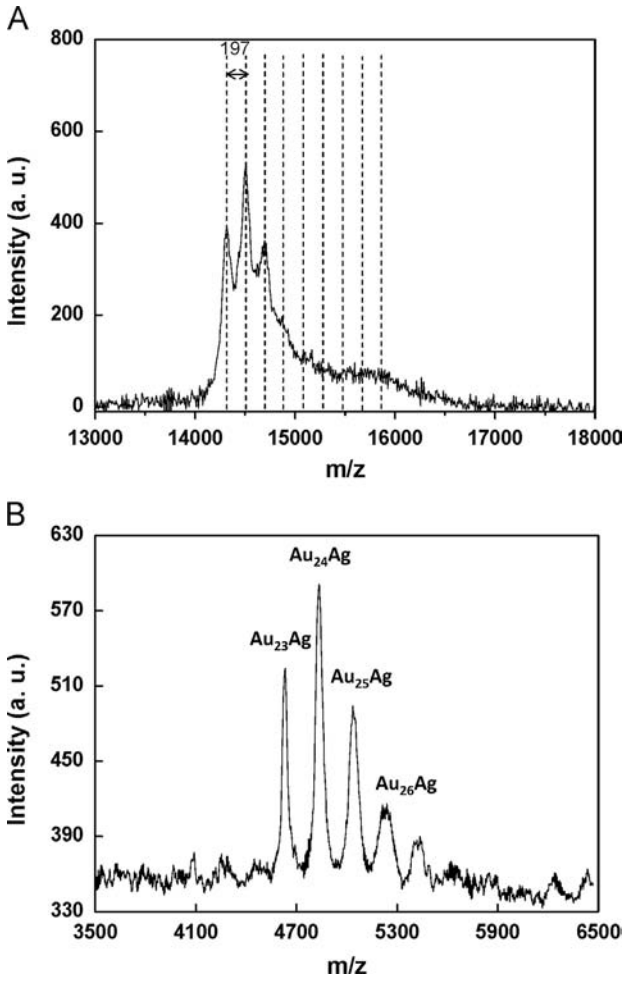

Fig. 2. MALDI-TOF mass spectra of (A) small- and (B) large-sized clusters.

respectively. Because the AuNCs preferentially consisted of a magic number of atoms (2, 8, 11, 13, 18, 22, 25, 28, 39, or 55) [24], large clusters were asserted to be $Au_{24}Ag$ magic clusters. Previous studies reported that Au–Ag bimetallic clusters consist of a $Au_{13-n}Ag_n$ bimetallic core and six [–S–Au–S–Au–S–] oligomers [25]. This is attributed to the deposition of a Ag atom on the surface of the M_{13} core being more energetically stable than the Ag atom contained in the oligomer. Based on previous results and our observations, the reduction of Ag^{+} on the Au surface could occur in the intermediate stage when Au^{+}–Lys VI complexes were converted to $Au_{24}Ag$ clusters. Small sizes were suggested to be the result of Au_7Ag and Au_8 clusters. XPS was used to determine the in-depth chemical state of two-sized clusters. The XPS spectrum obtained from dried clusters showed a peak indicative of Au $4f_{7/2}$ at 84.4 eV, which is higher than the value of the binding energy of Au(0) film (84.0 eV). Relative to the binding energy of Ag(0) film (368.3 eV), the binding energy of Ag $3d_{5/2}$ shifted to 368.1 eV. Previous studies demonstrate that the formation of Au–Ag bimetallic clusters causes an increase and decrease in binding energies of Au $4f_{7/2}$ and Ag $3d_{5/2}$, respectively [26,27]. These results and previous studies support the formation of Au–Ag bimetallic clusters.

3.2. Growth mechanism

Fig. S6 (Supplementary information) shows time-dependent fluorescent spectra of a mixture of Lys VI (25 mg/mL), $HAuCl_4$ (8 mM), and $AgNO_3$ (2 mM) when incubated at 37 °C at pH 12. With an increase in the reaction time from 2 to 18 h, the reduction in the fluorescence peak at 471 nm indicates that small clusters were converted to larger

clusters [13]. A shift in fluorescence maximum from 568 to 613 nm could reflect that the number of [–S–Au–S–Au–S–] oligomers gradually increased over time. Compared to the conversion of Au_8 clusters to Au_{25} clusters [13], the presence of Ag in the M_{13} core could slow down the formation of [–S–Au–S–Au–S–] oligomers. These results show that the reduction in fluorescence and the shift in the fluorescence peak were complete after 18 h. Previous studies have stated that the time for the synthesis of Au_{25} clusters was approximately 13 h [13]. The addition of Ag^+ to the precursor solution can clearly decelerate the conversion of small clusters to large clusters through the replacement of Au sites in AuNCs by Ag^+, thereby producing two-sized clusters.

3.3. Ratiometric sensing of Hg^{2+}

Previous studies have shown that Hg^{2+} can quench the fluorescence of Au_{25} clusters but not Au_8 clusters [6,13]. Thus, it is proposed that red-emitting $Au_{24}Ag$ clusters (denoted as Au-613) can selectively recognize Hg^{2+} through the formation of metallophilic bonding between Hg^{2+} and Au^+, leading to red fluorescence quenching, whereas the blue fluorescence of small clusters (Au_7Ag and Au_8; denoted as Au-471) remain constant because of the absence of Au^+ on the AuNC surface. When adding 100 nM Hg^{2+} to a solution containing two-sized clusters, a significant decrease in fluorescence at 613 nm ($I_{613\ nm}$) of Au-613 and an unchanged fluorescence at 471 nm ($I_{471\ nm}$) of Au-471 were observed (Fig. S7, Supplementary information). This result affords two-sized clusters a sensitive ratiometric fluorescent sensor for Hg^{2+}. With increasing incubation time between two-sized clusters and 100 nM Hg^{2+}, the fluorescence from the Au-613 quenched completely after 15 min and the fluorescence from the Au-471 remained nearly constant (Fig. S8, Supplementary information). By increasing the concentration of Hg^{2+}, the fluorescence spectra of the Au-613 showed a gradual decrease in fluorescence at 613 nm and no significant change ($<5\%$) in the fluorescence of Au-471 when increasing the Hg^{2+} concentration (Fig. 3A and B). By plotting the intensity ratio of the two emission wavelengths ($I_{613\ nm}/I_{471\ nm}$) against the concentrations of Hg^{2+}, two linear ranges were obtained from 6 to 100 nM ($R^2=0.9956$) and from 0.8 to 10 μM ($R^2=0.9964$) (inset in Fig. 3A and B). Two linear ranges obtained from this sensor is probably due to the fact that high concentration of Hg^{2+} reacts with two-sized clusters faster than low concentration of Hg^{2+}. The limit of detection (LOD) at an S/N ratio of 3 (98.3% confidence level) for Hg^{2+} was estimated to be 1 nM. In contrast, a calibration curve ($R^2=0.9541$) obtained by plotting the fluorescence intensity at 613 nm of the Au-613 against the Hg^{2+} concentrations was unable to be used for the quantification of Hg^{2+} (Fig. S9, Supplementary information). A rare change ($<10\%$) in the value of $I_{613\ nm}/I_{471\ nm}$ was observed under 400 nm excitation to approximately 4 h, reflecting that this probe can provide a built-in correction for photobleaching (Fig. S10, Supplementary material).

The selectivity of the proposed ratiometric sensor toward Hg^{2+} was tested next. Fig. 4 shows that change in the value of $I_{613\ nm}/I_{471\ nm}$ occurs within 15 min after separately adding Hg^{2+} (100 nM) and other metal ions (5000 nM) to a solution containing two-sized clusters. Clearly, only Hg^{2+} caused a significant change in the value of $I_{613\ nm}/I_{471\ nm}$, suggesting that the selectivity of the proposed ratiometric sensor is more than 50-fold for Hg^{2+} over any of the metal ions. Because nitroaromatic derivatives and H_2O_2 are known to quench the nanoparticle fluorescence [28,29], the fluorescence of this probe was measured in the presence of nitrobenzene and H_2O_2. Fig. S11 (Supplementary information) displays that this probe is highly selective to Hg^{2+} as compared to nitrobenzene and H_2O_2. We evaluated the feasibility this probe in detecting Hg^{2+} in tap water.

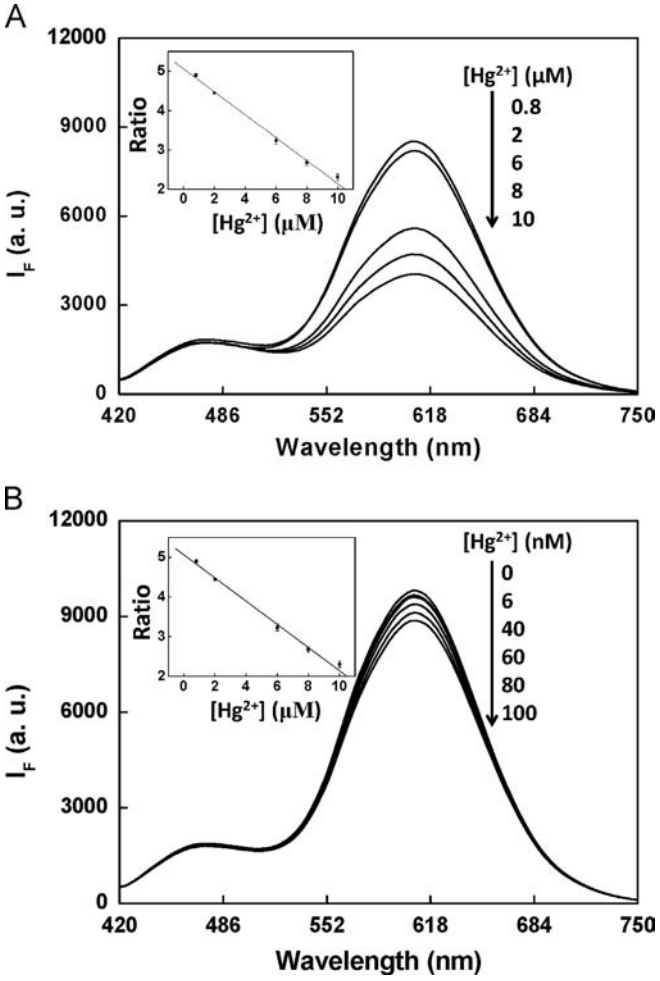

Fig. 3. Fluorescence spectra of a solution of two sized clusters in the presence of (A) 0.8–10 μM and (B) 0–100 nM Hg^{2+}. The arrows indicate the signal changes as increases in analyte concentrations. Inset: a plot of the values of $I_{613\ nm}/I_{471\ nm}$ versus the concentrations of Hg^{2+}. The excitation wavelength was set to 400 nm. The incubation time was 15 min. The error bars represent standard deviations based on three independent measurements.

The concentrations of total dissolved solids and total suspended solids in tap water were 323.4 and 3.3 mg/L, respectively. The conductivity and pH of tap water were 400 μS/cm and 7.8, respectively. An apparent reduction in fluorescence at 613 nm, and a rare change in fluorescence at 471 nm were observed after samples of tap water were spiked with standard solutions containing a series of Hg^{2+} concentrations (Fig. S12, Supplementary information). By plotting the value of $I_{613\ nm}/I_{471\ nm}$ versus the concentration of Hg^{2+}, the linear calibration curve ($R^2=0.994$) for quantifying Hg^{2+} in tap water was constructed from 6 to 80 nM (inset in Fig. S12, Supplementary information). The LOD of Hg^{2+} was 1 nM, which is lower than the maximum level (2 ppb; 10 nM) of mercury in drinking water permitted by the United States Environmental Protection Agency. Additionally, the proposed ratiometric sensor and ICP-MS were used to determine the spiked concentration of Hg^{2+} (30 nM) in tap water. By applying standard addition, the concentrations of Hg^{2+} in tap water determined by the proposed ratiometric sensor and ICP-MS were 28 ± 5 nM ($n=3$) and 30 ± 1 nM ($n=3$), respectively. Based on a t-test (95% confidence level, 4 degrees of freedom) and F-test (95% confidence level), the result obtained by the proposed probe was consistent with determined by ICP-MS. These results show that the proposed ratiometric sensor is applicable to the determination of Hg^{2+} in environmental water samples.

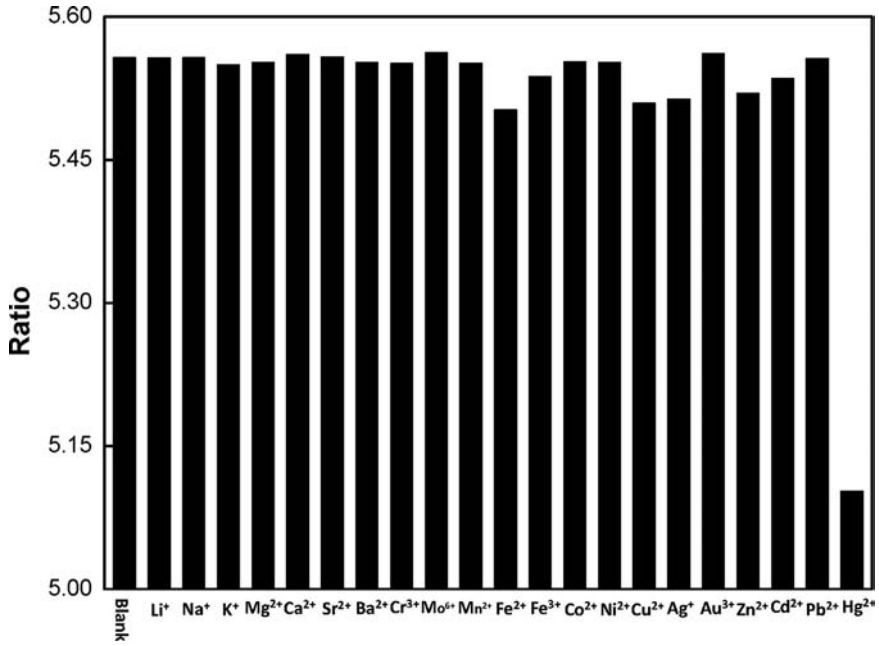

Fig. 4. Ratiometric fluorescence intensities ($I_{613\ nm}/I_{471\ nm}$) of solutions of two sized clusters after the addition of Hg^{2+} (100 nM) and other metal ions (5000 nM). The excitation wavelength was set to 400 nm. The incubation time was 15 min.

4. Conclusions

We developed a straightforward one-pot protocol for the preparation of two-sized clusters through the reduction of $HAuCl_4$ and $AgNO_3$ with Lys VI. The formation of $Au_{24}Ag$ clusters was confirmed using MALDI-TOF-MS. A probe containing two-sized clusters was designed as a ratiometric sensor to determine Hg^{2+} in environmental water. This is the first example of the use of metal-based nanoclusters for selective and sensitive ratiometric detection of Hg^{2+}. Photobleaching of two-sized clusters can be corrected by monitoring the fluorescence intensity ratio of Au-613 to Au-471. The synthesis protocol is expected to be applicable to other bimetallic clusters (e.g., PtAu).

Acknowledgments

We would like to thank the National Science Council (NSC 100-2628-M-110-001-MY4) for the financial support of this study. We also thank National Sun Yat-sen University and Center for Nanoscience and Nanotechnology for the measurement of fluorescence spectrum.

Appendix A. Supplementary material

Supplementary data associated with this article can be found in the online version at http://dx.doi.org/10.1016/j.talanta.2013.08.057.

References

[1] E.M. Nolan, S.J. Lippard, Chem. Rev. 108 (2008) 3443.
[2] X.F. Liu, Y.L. Tang, L.H. Wang, J. Zhang, S.P. Song, C.H. Fan, S. Wang, Adv. Mater. 19 (2007) 1471.
[3] Z.H. Wu, J.H. Lin, W.L. Tseng, Biosens. Bioelectron. 34 (2012) 185.
[4] J. Liu, Y. Lu, Angew. Chem. Int. Ed. 46 (2007) 7587.
[5] L.E. Page, X. Zhang, A.M. Jawaid, P.T. Snee, Chem. Commun. 47 (2011) 7773.
[6] Y.-H. Lin, W.-L. Tseng, Anal. Chem. 82 (2010) 9194.
[7] C.-C. Huang, Z. Yang, K.-H. Lee, H.-T. Chang, Angew. Chem. Int. Ed. 46 (2007) 6824.
[8] J. Xie, Y. Zheng, J.Y. Ying, Chem. Commun. 46 (2010) 961.
[9] A. Zhu, Q. Qu, X. Shao, B. Kong, Y. Tian, Angew. Chem. Int. Ed. 51 (2012) 7185.
[10] Y. Bao, B. Liu, H. Wang, J. Tian, R. Bai, Chem. Commun. 47 (2011) 3957.
[11] J. Wu, Y. Zou, C. Li, W. Sicking, I. Piantanida, T. Yi, C. Schmuck, J. Am. Chem. Soc. 134 (2012) 1958.
[12] K. Zhang, H. Zhou, Q. Mei, S. Wang, G. Guan, R. Liu, J. Zhang, Z. Zhang, J. Am. Chem. Soc. 133 (2011) 8424.
[13] T.-H. Chen, W.-L. Tseng, Small 8 (2012) 1912.
[14] M.Z. Liu, P. Guyot-Sionnest, J. Phys. Chem. B 109 (2005) 22192.
[15] M.L. Personick, M.R. Langille, J. Zhang, C.A. Mirkin, Nano Lett. 11 (2011) 3394.
[16] T. Ming, W. Feng, Q. Tang, F. Wang, L. Sun, J. Wang, C. Yan, J. Am. Chem. Soc. 131 (2009) 16350.
[17] C.-C. Huang, H.-Y. Liao, Y.-C. Shiang, Z.-H. Lin, Z. Yang, H.-T. Chang, J. Mater. Chem. 19 (2009) 755.
[18] T. Huang, R.W. Murray, J. Phys. Chem. B 107 (2003) 7434.
[19] J.S. Mohanty, P.L. Xavier, K. Chaudhari, M.S. Bootharaju, N. Goswami, S.K. Pal, T. Pradeep, Nanoscale 4 (2012) 4255.
[20] Z. Wu, M. Wang, J. Yang, X. Zheng, W. Cai, G. Meng, H. Qian, H. Wang, R. Jin, Small 8 (2012) 2028.
[21] J. Zheng, P.R. Nicovich, R.M. Dickson, Annu. Rev. Phys. Chem. 58 (2007) 409.
[22] H. Duan, S. Nie, J. Am. Chem. Soc. 129 (2007) 2412.
[23] Y. Bao, C. Zhong, D.M. Vu, J.P. Temirov, R.B. Dyer, J.S. Martinez, J. Phys. Chem. C 111 (2007) 12194.
[24] P. Pyykko, Nat. Nanotechnol. 2 (2007) 273.
[25] Y. Negishi, T. Iwai, M. Ide, Chem. Commun. 46 (2010) 4713.
[26] T. Endo, T. Yoshimura, K. Esumi, J. Colloid Interf. Sci. 286 (2005) 602.
[27] M.J. Kim, H.J. Na, K.C. Lee, E.A. Yoo, M.Y. Lee, J. Mater. Chem. 13 (2003) 1789.
[28] W. Chen, N.B. Zuckerman, J.P. Konopelski, S.W. Chen, Anal. Chem. 82 (2010) 461.
[29] F. Wen, Y.H. Dong, L. Feng, S. Wang, S.C. Zhang, X.R. Zhang, Anal. Chem. 83 (2011) 1193.